



New method to determine optimum impedance of fault current limiters for symmetrical and/or asymmetrical faults in power systems

Mahmoud MODARESI¹, Hamid LESANI^{‡2}

¹Department of Electrical Engineering, Science and Research Branch, Islamic Azad University, Tehran, Iran

²School of Electrical and Computer Engineering, University of Tehran, Tehran, Iran

E-mail: m.modaresi@srbiau.ac.ir; lesani@ut.ac.ir

Received Nov. 6, 2016; Revision accepted Apr. 17, 2017; Crosschecked Feb. 15, 2018

Abstract: To select the type and value of the impedance of fault current limiters (FCLs) for power network designers, we introduce a new method to calculate the optimum value of FCL impedance depending on its position in the network. Due to the complexity of its impedance, the costs of both real and imaginary parts of FCL impedance are considered. The optimization of FCL impedance is based on a goal function that maximizes the reduction of the fault current while minimizing the costs. While the position of FCL in the network has an effect on the calculation of the optimum impedance value, the method for selecting FCL location is not the focus of this study. The proposed method for optimizing FCL impedance can be used for every network that has symmetrical and/or asymmetrical faults. We use a 14-bus IEEE network as an example to explain the process. The optimum FCL impedance used in this network is calculated by considering the vast range of costs for both real and imaginary parts of FCL impedance.

Key words: Fault current limiter (FCL); FCL impedance; Short circuit current; Fault current; Power system
<https://doi.org/10.1631/FITEE.1601689>

CLC number: TM77

1 Introduction

Increasing the fault currents has been a big challenge in power systems (Nagata et al., 2001; Hongesombut et al., 2003; Kovalsky et al., 2005; Teng and Lu, 2010; Javadi, 2011; Abramovitz and Smedley, 2012; Fotuhi-Firuzabad et al., 2012; Alaraifi et al., 2013). To decrease the fault current level, one method increases Thevenin's equivalent impedance by splitting bus ties of substations or by adding series reactors to the network. However, this process increases the system loss and can also decrease the voltage and the stability of the network

(Kovalsky et al., 2005; Javadi, 2011; Abramovitz and Smedley, 2012; Fotuhi-Firuzabad et al., 2012; Alaraifi et al., 2013; El Moursi and Hegazy, 2013; Naderi et al., 2013).

Another method uses a fault current limiter (FCL) to reduce the fault current as a result of adding impedance to the system. The FCL impedance in normal conditions is nearly zero, but when a fault occurs in the network, the impedance changes to Z_{FCL} (Mukhopadhyay et al., 1998; Kovalsky et al., 2005; Cvoric et al., 2010; Javadi, 2011; Abramovitz and Smedley, 2012; Fotuhi-Firuzabad et al., 2012; Shahriari et al., 2012; Alaraifi et al., 2013; El Moursi and Hegazy, 2013; Naderi et al., 2013). Fig. 1 shows the FCL configuration before and after fault occurrence.

Depending on the mechanism and the time of adding or removing FCL impedance, there are many

[‡] Corresponding author

ORCID: Mahmoud MODARESI, <http://orcid.org/0000-0003-1020-1554>

© Zhejiang University and Springer-Verlag GmbH Germany, part of Springer Nature 2018

FCL types such as superconductor FCL (SFCL) (Nagata et al., 2001; Hongesombut et al., 2003; Kovalsky et al., 2005; Stemmler et al., 2007; Yamaguchi and Kataoka, 2007; Alaraifi et al., 2013; El Moursi and Hegazy, 2013; Didier and L ev eque, 2014), series or parallel resonance FCL (Javadi, 2011; Naderi et al., 2013), magnetic FCL (Mukhopadhyay et al., 1998; Cvoric et al., 2010), and solid state FCL (Abramovitz and Smedley, 2012; Shahriari et al., 2012; Hossen Heidary et al., 2015). In these types of FCL, the impedance can be resistance (R_{FCL}), inductive reactance (X_{FCL}^L), capacitive reactance (X_{FCL}^C), or a complex value that is a combination of any or all of them (Hossen Heidary et al., 2015).

During fault occurrence, the FCL impedance can be either a fixed value or a variable value. For the FCLs with variable impedance, such as SFCLs, impedance increases rapidly until it reaches the maximum value (Nagata et al., 2001; Abramovitz and Smedley, 2012; Alaraifi et al., 2013; El Moursi and Hegazy, 2013; Didier and L ev eque, 2014). In such cases, the maximum value of FCL impedance is important for calculating optimum impedance (Nagata et al., 2001; Didier and L ev eque, 2014).

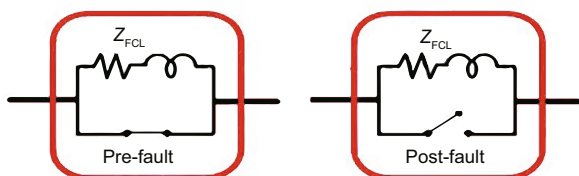


Fig. 1 Circuitual representation of the fault current limiter at pre- and post-fault periods

The FCL impedance increases when the cost of FCL rises (Nagata et al., 2001; Hongesombut et al., 2003; Teng and Lu, 2010), and the level of fault current decreases until it levels off, if the FCL impedance increases (Stemmler et al., 2007; Yamaguchi and Kataoka, 2007; El Moursi and Hegazy, 2013; Didier et al., 2015). In the power network, the fault current of buses should be less than the maximum allowable current (I_m) of circuit breakers and other components of the network (Nagata et al., 2001; Hongesombut et al., 2003; Teng and Lu, 2010; Dam et al., 2013). The selection of the value and the type of FCL impedance is a big challenge for network designers.

In previous work (Nagata et al., 2001; Hongesombut et al., 2003; Teng and Lu, 2010), the impedance of FCL was selected based on the lower value of FCL impedance, providing that the fault currents of all buses of a network are equal to or less than I_m . However, this approach inevitably cannot be the optimal option because if the fault current can be further reduced, it can have a positive effect on the network. For example, it can reduce the failure probability of the network components and increase the system reliability (Dam and Meliopoulos, 2006, 2007; Haghifam et al., 2009; Kim et al., 2010, 2011, 2012; Dam et al., 2013; Yousefi et al., 2016). It can also reduce the level of electro-mechanical and thermal tensions on network components (Hongesombut et al., 2003; Cvoric et al., 2010; Abramovitz and Smedley, 2012; Fotuhi-Firuzabad et al., 2012). Therefore, the ability to reduce fault current can be an important criterion in the selection of FCL impedance.

In other cases (Nagata et al., 2001; Hongesombut et al., 2003; Seo et al., 2010; Teng and Lu, 2010; Alaraifi et al., 2013), the FCL impedance has been simply chosen to be purely R_{FCL} or purely X_{FCL}^L , and then the optimum value of FCL impedance is determined. The FCL impedance can be generally a complex value, consisting of the real and imaginary parts (Guo et al., 2001; Matsumura et al., 2001). Therefore, different costs of the real and imaginary parts of FCL impedance can affect the selection of the value and type of FCL impedance.

In this study, an approach is proposed to calculate the optimum FCL impedance for power networks. To be neutral, the FCL impedance can be assumed to be a complex value consisting of R_{FCL} , X_{FCL}^L , and X_{FCL}^C . Depending on the network data and the type of fault (three-phase-symmetrical (3ph) or single-line-to-ground (1ph)), the fault currents are calculated. By considering both the higher fault current reduction and the lower cost of FCL, the optimum value of FCL impedance is determined at a certain location in the network. The results are then verified using a computer program developed for the 14-bus IEEE system.

Note that FCL positioning is not the main goal of this study, but it can be taken into account in future studies. In addition, the mechanism of FCL operation is not the objective of this study and only the FCL impedance value after fault occurrence is considered.

2 Fault current before and after FCL installation

Generally, different kinds of faults in a system include 3ph, line-to-line, double-line-to-ground, and 1ph faults. 3ph and 1ph faults are of great importance in network study (Stemmler et al., 2007; Dam et al., 2013).

2.1 Fault current before FCL installation

Assuming that the fault impedance is Z_f , 3ph fault currents (I_f^{3ph}) and 1ph fault currents (I_f^{1ph}) are calculated by (Saadat, 1999)

$$I_f^{3ph} = V_f / Z_{ff}^+ + Z_f, \quad (1)$$

$$I_f^{1ph} = 3V_f / Z_{ff}^0 + Z_{ff}^+ + Z_{ff}^- + 3Z_f. \quad (2)$$

V_f is the voltage of bus f before fault occurrence, Z_{ff}^0 , Z_{ff}^+ , and Z_{ff}^- are Thevenin's impedance of zero, positive, and negative sequences to be achieved from the impedance matrix of the network, respectively. To calculate the worst fault current, Z_f is assumed to be zero.

2.2 Fault current after FCL installation

If there is a need to install an FCL in bus i of a power network, bus i is divided into two parts as buses i_A and i_B , and the FCL is placed between them. Components A and B are equivalent to components connected to buses i_A and i_B , respectively, in Figs. 2a–2c.

In this case, the impedance matrix for an n -bus network after separating buses and before FCL installation is represented by Eq. (3), and the impedance matrix after FCL installation is represented by Eq. (4). Each matrix element in Eq. (4) is calculated by Eq. (5) (Saadat, 1999).

$$Z_{Bus} = \begin{bmatrix} Z_{11} & \dots & Z_{1i_A} & Z_{1i_B} & \dots & Z_{1n} \\ \vdots & & \vdots & \vdots & & \vdots \\ Z_{i_A 1} & \dots & Z_{i_A i_A} & Z_{i_A i_B} & \dots & Z_{i_A n} \\ Z_{i_B 1} & \dots & Z_{i_B i_A} & Z_{i_B i_B} & \dots & Z_{i_B n} \\ \vdots & & \vdots & \vdots & & \vdots \\ Z_{n1} & \dots & Z_{ni_A} & Z_{ni_B} & \dots & Z_{nn} \end{bmatrix}, \quad (3)$$

$$Z_{Bus}^{new} = \begin{bmatrix} Z_{11}^{new} & \dots & Z_{1i_A}^{new} & Z_{1i_B}^{new} & \dots & Z_{1n}^{new} \\ \vdots & & \vdots & \vdots & & \vdots \\ Z_{i_A 1}^{new} & \dots & Z_{i_A i_A}^{new} & Z_{i_A i_B}^{new} & \dots & Z_{i_A n}^{new} \\ Z_{i_B 1}^{new} & \dots & Z_{i_B i_A}^{new} & Z_{i_B i_B}^{new} & \dots & Z_{i_B n}^{new} \\ \vdots & & \vdots & \vdots & & \vdots \\ Z_{n1}^{new} & \dots & Z_{ni_A}^{new} & Z_{ni_B}^{new} & \dots & Z_{nn}^{new} \end{bmatrix}, \quad (4)$$

$$Z_{jk}^{new} = Z_{jk} - \frac{(Z_{ji_A} - Z_{ji_B})(Z_{i_A k} - Z_{i_B k})}{Z_{i_A i_A} + Z_{i_B i_B} - 2Z_{i_A i_B} + Z_{FCL}}. \quad (5)$$

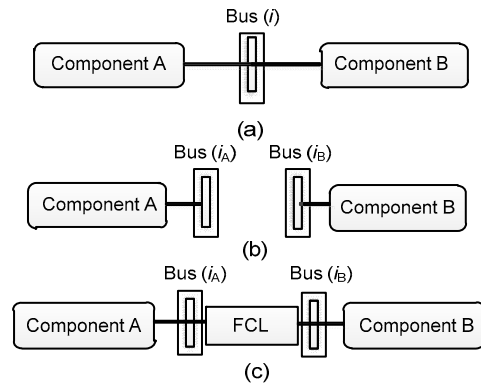


Fig. 2 Bus i before separating the bus (a), after separating the bus (b), and after FCL installation (c)

If bus f is the goal of fault current calculation and an FCL is installed between buses i_A and i_B , a general form of I_f^{3ph} and I_f^{1ph} for bus f is represented by Eqs. (6) and (7), respectively:

$$I_f^{3ph} = A \cdot \frac{Z_{FCL} + B}{Z_{FCL} + C}, \quad (6)$$

$$I_f^{1ph} = D \cdot \frac{Z_{FCL}^2 + EZ_{FCL} + F}{Z_{FCL}^2 + GZ_{FCL} + H}, \quad (7)$$

where variables A , B , C , D , E , F , G , and H are calculated by Eqs. (8)–(15) using the elements driven by the impedance matrix of zero, positive, and negative sequences, with j equal to $\sqrt{-1}$.

$$A = V_f / Z_{ff}^+ = A_1 + jA_2 = |A| \angle \theta_A, \quad (8)$$

$$B = Z_{i_A i_A}^+ + Z_{i_B i_B}^+ - 2Z_{i_A i_B}^+ = B_1 + jB_2, \quad (9)$$

$$C = B + 2Z_{f i_A}^+ Z_{f i_B}^+ - Z_{f i_A}^+ Z_{i_A f}^+ - Z_{f i_B}^+ Z_{i_B f}^+ / Z_{ff}^+ = C_1 + jC_2, \quad (10)$$

$$D = 3V_f / Z_{ff}^0 + 2Z_{ff}^+ = D_1 + jD_2 = |D| \angle \theta_D, \quad (11)$$

$$E = L + N = E_1 + jE_2, \quad (12)$$

$$F = LN = F_1 + jF_2, \quad (13)$$

$$G = E - (K + M) / (Z_{ff}^0 + 2Z_{ff}^+) = G_1 + jG_2, \quad (14)$$

$$H = F - (KN + ML) / (Z_{ff}^0 + 2Z_{ff}^+) = H_1 + jH_2. \quad (15)$$

In Eqs. (12)–(15), the elements of K , L , M , and N are expressed by

$$K = (Z_{f_A}^0 - Z_{f_B}^0)(Z_{i_A f}^0 - Z_{i_B f}^0), \quad (16)$$

$$L = Z_{i_A i_A}^0 + Z_{i_B i_B}^0 - 2Z_{i_A i_B}^0, \quad (17)$$

$$M = 2(Z_{f_A}^+ - Z_{f_B}^+)(Z_{i_A f}^+ - Z_{i_B f}^+), \quad (18)$$

$$N = Z_{i_A i_A}^+ + Z_{i_B i_B}^+ - 2Z_{i_A i_B}^+. \quad (19)$$

Z_{FCL} is called FCL impedance. According to Eq. (20), it includes a real part R_{FCL} and an imaginary part X_{FCL} . R_{FCL} is FCL resistance and is always positive, but X_{FCL} is FCL reactance and can be either positive or negative, depending on X_{FCL}^L or X_{FCL}^C .

$$Z_{FCL} = R_{FCL} + jX_{FCL}. \quad (20)$$

The current magnitude of 3ph fault ($|I_f^{3ph}|$) and the current magnitude of 1ph fault ($|I_f^{1ph}|$) for bus f can be calculated by Eqs. (21) and (22), where O , P , T , and U are expressed by Eqs. (23)–(26):

$$|I_f^{3ph}| = |A| \sqrt{\frac{(R_{FCL} + B_1)^2 + (X_{FCL} + B_2)^2}{(R_{FCL} + C_1)^2 + (X_{FCL} + C_2)^2}}, \quad (21)$$

$$|I_f^{1ph}| = |D| \sqrt{\frac{O^2 + P^2}{T^2 + U^2}}, \quad (22)$$

$$O = R_{FCL}^2 - X_{FCL}^2 + R_{FCL}E_1 - X_{FCL}E_2 + F_1, \quad (23)$$

$$P = 2R_{FCL}X_{FCL} + R_{FCL}E_2 + X_{FCL}E_1 + F_2, \quad (24)$$

$$T = R_{FCL}^2 - X_{FCL}^2 + R_{FCL}G_1 - X_{FCL}G_2 + H_1, \quad (25)$$

$$U = 2R_{FCL}X_{FCL} + R_{FCL}G_2 + X_{FCL}G_1 + H_2. \quad (26)$$

3 FCL impedance locus and its cost function

3.1 FCL impedance locus regarding I_m of buses

The fault current passing through the components of the network should be equal to or less than the

maximum total allowable current (I_m) of the network components. The FCL impedance locus is the acceptable range of FCL impedance, which causes the fault current magnitude of a given bus to be equal to or less than I_m for the same bus on that network.

The FCL impedance locus for the 3ph fault is calculated by $|I_f^{3ph}| = I_m$ by

$$\left(R_{FCL} + \frac{M^2 C_1 - B_1}{M^2 - 1} \right)^2 + \left(X_{FCL} + \frac{M^2 C_2 - B_2}{M^2 - 1} \right)^2 = \left(\frac{M \sqrt{(C_1 - B_1)^2 + (C_2 - B_2)^2}}{M^2 - 1} \right)^2, \quad (27)$$

where $M = I_m / |A|$.

Eq. (27) represents a circle (Fig. 3) for a test system. If $M > 1$, the loci of R_{FCL} and X_{FCL} are outside the circle area; if $M < 1$, they are inside the circle area. In Fig. 3, R_C is the radius of the circle and D_C is the distance from the center to the origin. Note that R_{FCL} is resistance and actually cannot be a negative value.

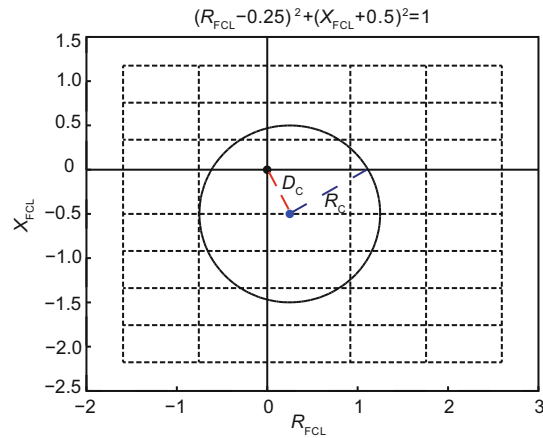


Fig. 3 The FCL impedance locus for fault current equal to I_m in a test system

The FCL impedance locus for 1ph fault can be mathematically calculated by $|I_f^{1ph}| = I_m$. However, for simplification, the calculations are not shown here.

3.2 Cost function of FCL impedance

The selection of FCL without considering the type or cost of FCL impedance cannot produce the optimal results. For example, regarding Fig. 3, if the costs of R_{FCL} , X_{FCL}^L , and X_{FCL}^C are the same, then X_{FCL}^L is the best selection due to the lower impedance

value compared to other types of FCL impedance. However, if the cost of X_{FCL}^L is three times that of R_{FCL} or more, then R_{FCL} is a better choice due to the lower cost of FCL.

The cost of an FCL includes both the real and imaginary parts of FCL impedance. The cost of each part rises as the value of the impedance increases (Nagata et al., 2001; Hongesombut et al., 2003; Teng and Lu, 2010). If $Cost_R^{FCL}$, $Cost_{X_L}^{FCL}$, and $Cost_{X_C}^{FCL}$ are the costs of each ohm (Ω) or per unit (p.u.) for R_{FCL} , X_{FCL}^L , and X_{FCL}^C , and $|R_{FCL}|$, $|X_{FCL}^L|$, and $|X_{FCL}^C|$ are the absolute values of R_{FCL} , X_{FCL}^L , and X_{FCL}^C respectively in Ω or p.u., then the cost of an FCL ($Cost_{eq}^{FCL}$) is obtained by

$$Cost_{eq}^{FCL} = |R_{FCL}| \cdot Cost_R^{FCL} + |X_{FCL}^L| \cdot Cost_{X_L}^{FCL} + |X_{FCL}^C| \cdot Cost_{X_C}^{FCL} \quad (28)$$

Dividing both sides of Eq. (28) by $Cost_R^{FCL}$ produces the cost function of FCL ($Z' = Cost_{eq}^{FCL} / Cost_R^{FCL}$) as shown in Eq. (29), and cost factors w_L and w_C are calculated by

$$Z' = |R_{FCL}| + w_L \cdot |X_{FCL}^L| + w_C \cdot |X_{FCL}^C|, \quad (29)$$

$$w_L = Cost_{X_L}^{FCL} / Cost_R^{FCL}, \quad (30)$$

$$w_C = Cost_{X_C}^{FCL} / Cost_R^{FCL}. \quad (31)$$

Network designers can select the proper w_L or w_C depending on their design priorities but not the cost of the parts of FCL impedance. Simultaneous use of X_{FCL}^L and X_{FCL}^C is not suitable because they cancel each other's effects. Therefore, the expression Z' is modified:

$$Z' = \begin{cases} R_{FCL} + w_L \cdot X_{FCL}^L, & \text{if } Z_{FCL} \text{ includes } R_{FCL} \text{ and } X_{FCL}^L, \\ R_{FCL} - w_C \cdot X_{FCL}^C, & \text{if } Z_{FCL} \text{ includes } R_{FCL} \text{ and } X_{FCL}^C. \end{cases} \quad (32)$$

4 Optimization of FCL impedance

Selection of FCL impedance based on the fault current of buses which is equal to I_m does not necessarily produce optimized results. It is possible to

have impedance that greatly reduces the fault current and it is also economically viable. Therefore, depending on $|I_f^{3ph}|$ and $|I_f^{1ph}|$, functions F^{3ph} and F^{1ph} are defined by Eqs. (33) and (34), respectively, which achieve FCL impedance based on the maximum reduction of fault current and the minimum cost of FCL.

$$F^{3ph} = |I_f^{3ph0}| - |I_f^{3ph}| / Z', \quad (33)$$

$$F^{1ph} = |I_f^{1ph0}| - |I_f^{1ph}| / Z', \quad (34)$$

where $|I_f^{3ph0}|$ and $|I_f^{3ph}|$ are the absolute values of the fault current of bus f before and after FCL installation (Eq. (21)), respectively, and $|I_f^{1ph0}|$ and $|I_f^{1ph}|$ are the absolute values of the fault current of bus f before and after FCL installation (Eq. (22)), respectively.

The functions F^{3ph} and F^{1ph} include variables R_{FCL} and X_{FCL} , which can be of different values. Therefore, assuming $|Z|$ is the absolute value of FCL impedance and θ its angle, R_{FCL} and X_{FCL} can be expressed by

$$R_{FCL} = |Z| \cos \theta, \quad (35)$$

$$X_{FCL} = |Z| \sin \theta. \quad (36)$$

θ can be varied between -90° and 90° . If $\theta > 0$, then $X_{FCL} = X_{FCL}^L$; if $\theta < 0$, then $X_{FCL} = X_{FCL}^C$. The Z' , R_{FCL} , X_{FCL} , and α are expressed by

$$Z' = \alpha |Z|, \quad (37)$$

$$R_{FCL} = Z' \cos \theta / \alpha, \quad (38)$$

$$X_{FCL} = Z' \sin \theta / \alpha, \quad (39)$$

$$\alpha = \begin{cases} \cos \theta + w_L \sin \theta, & 0^\circ \leq \theta \leq 90^\circ, \\ \cos \theta - w_C \sin \theta, & -90^\circ \leq \theta < 0^\circ. \end{cases} \quad (40)$$

Note that the function F^{1ph} can be calculated by Eq. (34). However, for simplification, the process of further expansion is shown only for 3ph fault:

$$F^{3ph} = \frac{|A|}{Z'} \left[\sqrt{\frac{B_1^2 + B_2^2}{C_1^2 + C_2^2}} - \sqrt{\frac{Z'^2 + 2\alpha Z'(B_1 \cos \theta + B_2 \sin \theta) + \alpha^2 (B_1^2 + B_2^2)}{Z'^2 + 2\alpha Z'(C_1 \cos \theta + C_2 \sin \theta) + \alpha^2 (C_1^2 + C_2^2)}} \right]. \quad (41)$$

The extreme points of function F^{3ph} can be calculated when θ and α determine a fixed value and the derivative of F^{3ph} with respect to Z' is set to zero. The number of extreme points Z' in Eq. (41) is 8. Among the calculated values of Z' , the higher the value of F^{3ph} , the better the FCL impedance. However, the maximum F^{3ph} is not necessarily the optimum option, because that impedance may not resolve the I_m limitation of buses. If none of the selected Z' can decrease the fault current to a level equal to or less than I_m , this problem can be solved by increasing the Z' according to the FCL impedance locus. The new Z' (Z'_{new}) is expressed as

$$Z'_{new}{}^2 - 2Z'_{new} D_C \cos \theta + D_C^2 - R_C^2 = 0. \quad (42)$$

So far, the achieved Z' is calculated using the specific θ . However, to use various θ values, one can change θ at the range of $-90^\circ \leq \theta \leq 90^\circ$ and repeat FCL impedance optimization using the new θ , which allows calculation of the various values of Z' . Therefore, the optimal Z' can be selected by comparing the values of F^{3ph} for all Z' 's by Eq. (41). Note that a proper θ can be selected by a genetic algorithm or other methods; however, for simplification, θ is changed by step $\Delta\theta=0.1^\circ$. The smaller the increase in $\Delta\theta$ is, the more accurate the calculations of optimum FCL impedance will be. However, this can impact the computational time.

Finally, with the obtained values of Z' and θ , the real and imaginary parts of optimal FCL impedance are calculated by Eqs. (38) and (39), respectively. The computer algorithm for the proposed FCL impedance optimization is shown in Fig. 4.

With respect to Eq. (37) and by substituting $\alpha|Z|$ for Z' in Eq. (41), we have

$$F^{3ph} = \frac{|A|}{\alpha|Z|} \left[\sqrt{\frac{B_1^2 + B_2^2}{C_1^2 + C_2^2}} - \sqrt{\frac{|Z|^2 + 2|Z|(B_1 \cos \theta + B_2 \sin \theta) + (B_1^2 + B_2^2)}{|Z|^2 + 2|Z|(C_1 \cos \theta + C_2 \sin \theta) + (C_1^2 + C_2^2)}} \right]. \quad (43)$$

The extreme points of function F^{3ph} in Eq. (43) are calculated when θ is a fixed value and the derivative of the function F^{3ph} with respect to $|Z|$ is set to zero. When comparing the extreme points of

function F^{3ph} for Eqs. (41) and (43), it appears that the values of $|Z|$ and Z'/α at the extreme point of the function F^{3ph} are equal.

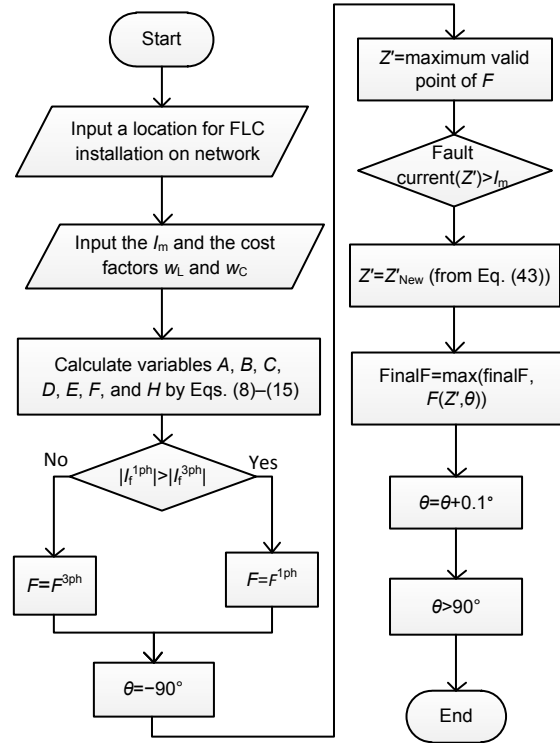


Fig. 4 Flowchart of the proposed FCL impedance optimization

The $|Z|$ is independent of w_L and w_C ; therefore, changing w_L and w_C does not affect the $|Z|$ for optimum FCL impedance when θ is a fixed value. This means that the value of Z'/α is unchanged within a specific range of w_L and w_C in a fixed θ .

It is interesting that different ranges of w_L and w_C affect the types of optimal FCL impedance, but they do not affect the optimal value of impedance in each case.

5 Numerical studies

5.1 Test system description

To achieve optimal FCL impedance, the proposed algorithm can be used for each power network. The IEEE 14-bus system (Fig. 5) is used for conducting FCL impedance optimization (Christie, 2012). The impedance data (R_a, X_d') of the generators and compensators are shown in Table 1.

Table 1 Impedance data of generators and compensators

Component	Bus No.	R_a (p.u.)	X_d' (p.u.)
Generators	1	0	0.23
	2	0.0031	0.23
	3	0.0031	0.13
Compensators	6	0.0014	0.12
	8	0.0014	0.12

$|I_f^{3ph}|$ is calculated for all buses before FCL installation. The fault current of bus 2 equals 15.37 p.u., which is the highest value of $|I_f^{3ph}|$. According to Fig. 5, an FCL is placed on bus 2. The variables $|A|$, B_1 , B_2 , C_1 , and C_2 , considering the 3ph fault occurrence in bus 2, are calculated by Eqs. (8)–(10) and recorded in Table 2.

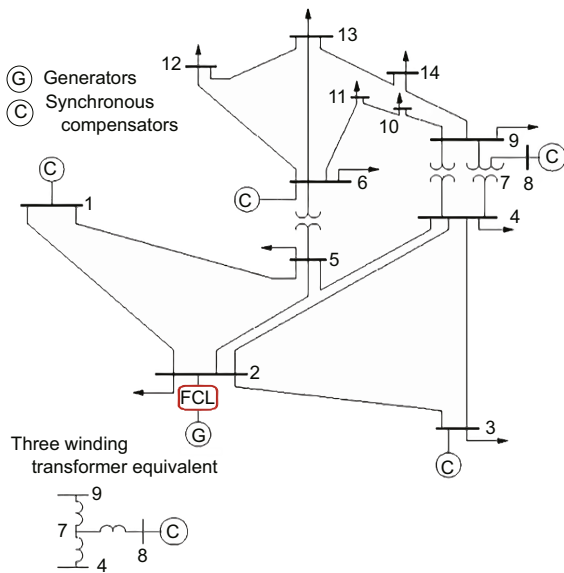


Fig. 5 IEEE 14-bus test system

Table 2 The variables $|A|$, B_1 , B_2 , C_1 , and C_2

$ A $	B_1	B_2	C_1	C_2
10.84	0.0145	0.3257	0.0031	0.23

Fig. 6 shows the $|I_f^{3ph}|$ for bus 2 versus the different ranges of FCL impedance including R_{FCL} and X_{FCL}^L . It shows that for FCL impedance with R_{FCL} and X_{FCL}^L , $|I_f^{3ph}|$ decreases as a homographic function and the minimum value of the fault current is equal to $|A|$, which will occur at an infinite value for FCL impedance.

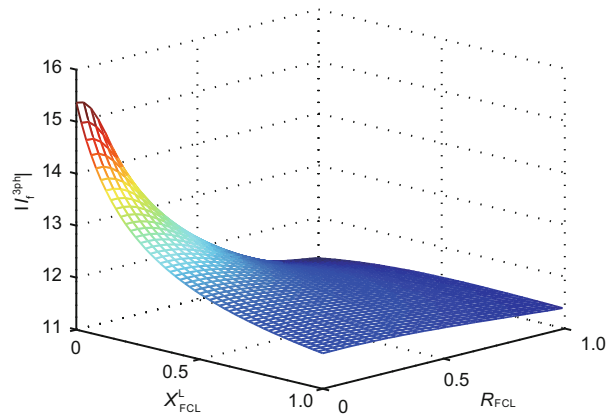


Fig. 6 Differentiation of $|I_f^{3ph}|$ versus FCL impedance (R_{FCL} and X_{FCL}^L)

Fig. 7 shows the $|I_f^{3ph}|$ for bus 2 versus the different ranges of FCL impedance including R_{FCL} and X_{FCL}^C . It is shown that for FCL impedance with R_{FCL} and X_{FCL}^C , the $|I_f^{3ph}|$ first reaches a peak and then decreases to a minimum. It then rises and reaches $|A|$ at an infinite value for FCL impedance.

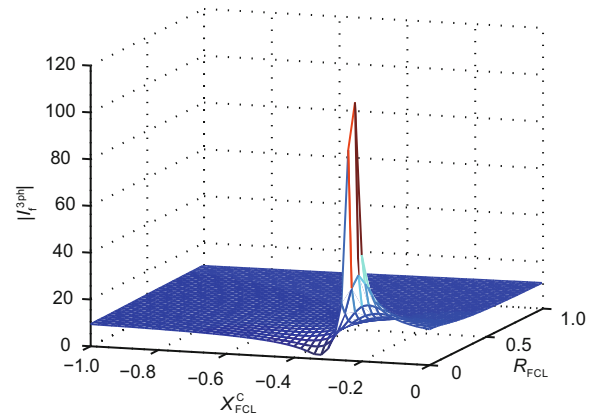


Fig. 7 Differentiation of $|I_f^{3ph}|$ versus FCL impedance (R_{FCL} and X_{FCL}^C) (References to color refer to the online version of this figure)

5.2 Test results and discussion

Depending on I_m , the acceptable FCL impedance locus is different. The FCL impedance optimization is conducted for two scenarios. In the first scenario, $I_m=11$ p.u. and the acceptable FCL impedance locus is shown in Fig. 8. In the second scenario, $I_m=14$ p.u. and its acceptable FCL impedance locus is shown in Fig. 9. Different colors in these figures show the different fault current magnitudes in p.u..

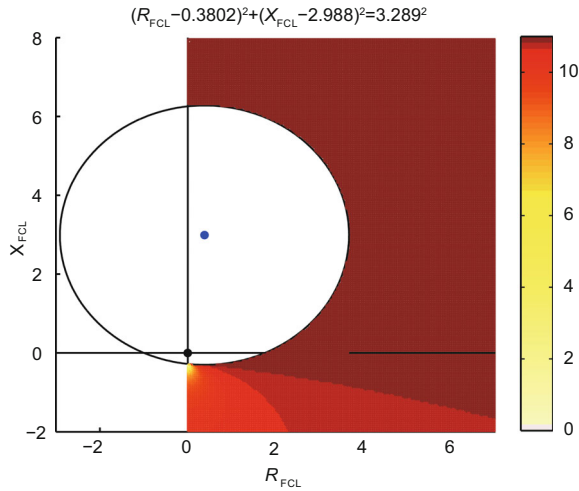


Fig. 8 FCL impedance locus for $I_m=11$ p.u. (References to color refer to the online version of this figure)

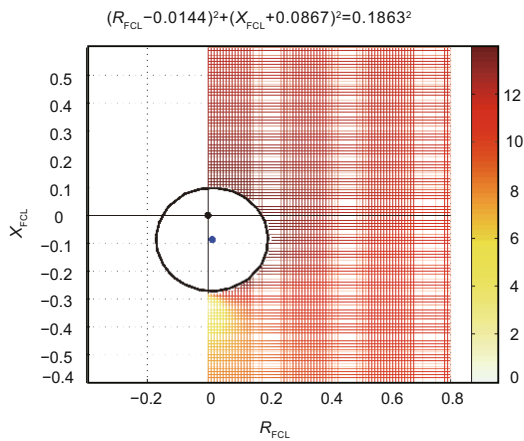


Fig. 9 The FCL impedance locus for $I_m=14$ p.u.

The costs of real and imaginary parts of impedance for different types of FCL can be different. The optimal FCL impedances for different ranges of w_L and w_C are calculated. The values of optimal R_{FCL} , X_{FCL} , and $|I_f^{3ph}|$ for $I_m=11$ p.u. are shown in Figs. 10a–10c, and those for $I_m=14$ p.u. are shown in Figs. 11a–11c. Tables 3 and 4 summarize all the related values used in Figs. 10 and 11.

1. At the optimal level of FCL impedance for both R_{FCL} and X_{FCL} , the $|I_f^{3ph}|$ is equal to I_m where $I_m=11$ p.u.. However, when $I_m=14$ p.u., the $|I_f^{3ph}|$ for optimal resistive FCL (R_{FCL}) is less than I_m . It shows that the selection of FCL impedance solely based on I_m limitation is not necessarily the optimum solution.

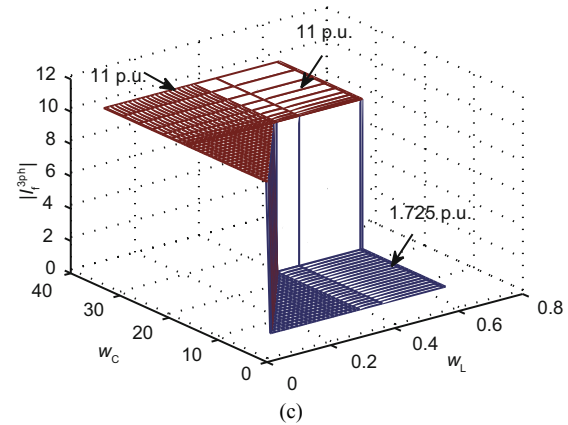
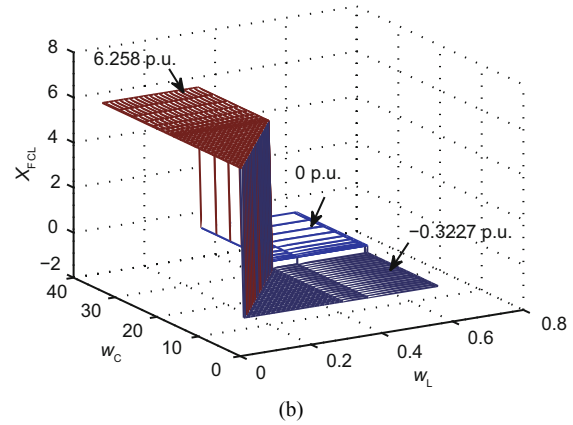
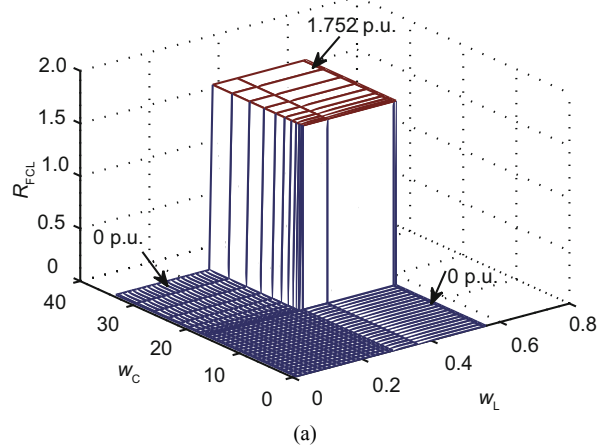


Fig. 10 R_{FCL} (a), X_{FCL} (b), and $|I_f^{3ph}|$ (c) for different ranges of w_L and w_C when $I_m=11$ p.u.

2. The highest reduction of fault current occurs for $I_m=11$ p.u. and $I_m=14$ p.u. when an X_{FCL}^C is selected for FCL. However, it is not necessarily the optimum solution due to different ranges of w_L and w_C . Note that using the X_{FCL}^C might cause some problems such as sub-synchronous resonance and instability in the power system. Therefore, to choose the capacitive

FCL, one should study the power system stability, which is out of the scope of this study and can be a basis for future studies.

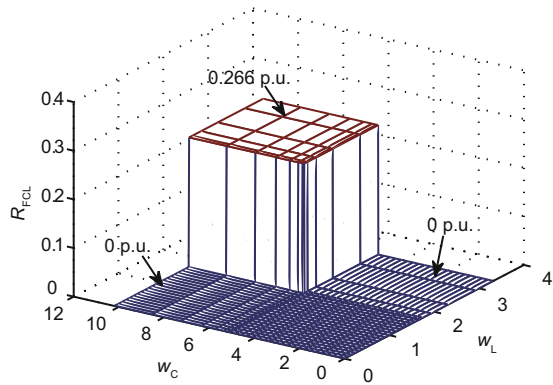
3. The optimal FCL impedance for different ranges of w_L and w_C is only one of the cases of R_{FCL} , X_{FCL}^L , or X_{FCL}^C . Thus, the combination of R_{FCL} and X_{FCL}^L or R_{FCL} and X_{FCL}^C for this network is not optimized.

4. The optimum impedance value for pure R_{FCL} , pure X_{FCL}^L , or pure X_{FCL}^C is a fixed value for each of

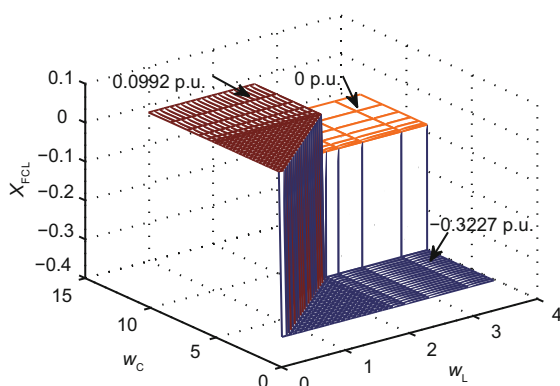
the above cases but a different value among all of those cases. It means that different ranges of w_L and w_C affect the type of optimal FCL impedance but do not affect the optimal value of impedance in each case.

Table 3 The optimal value of FCL impedance and $|I_f^{3ph}|$ for $I_m=11$ p.u. according to different ranges of w_L and w_C

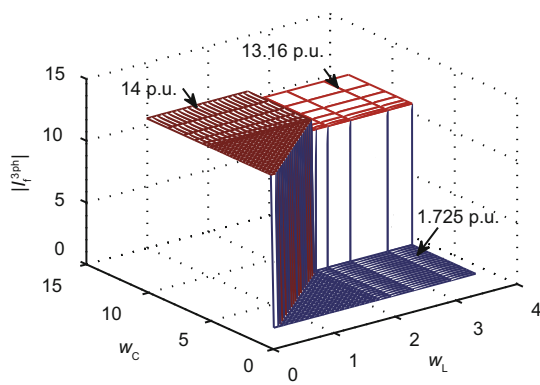
w_L	w_C	Z_{FCL} (p.u.)	$ I_f^{3ph} $ (p.u.)
>0.2795	>16.965	1.752	11
<0.2795	$>60.7w_L$	6.258i	11
$>0.0165w_C$	<16.965	-0.3227i	1.725



(a)



(b)



(c)

Fig. 11 R_{FCL} (a), X_{FCL} (b), and $|I_f^{3ph}|$ (c) for different ranges of w_L and w_C when $I_m=14$ p.u.

Figs. 12–15 show the values of Z' and Z'/α for various ranges of w_L and w_C for both cases including $I_m=11$ p.u. and $I_m=14$ p.u.. They show that the value of Z' varies but the value of Z'/α is definite for different ranges of w_L and w_C . Thus, the optimal FCL impedance is a fixed value when θ is fixed.

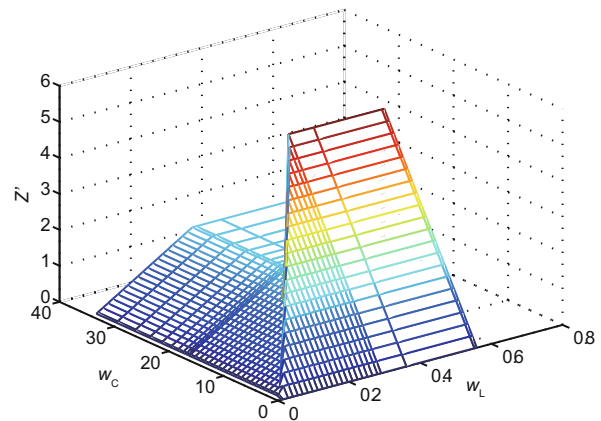


Fig. 12 Value of Z' for different ranges of w_L and w_C when $I_m=11$ kA

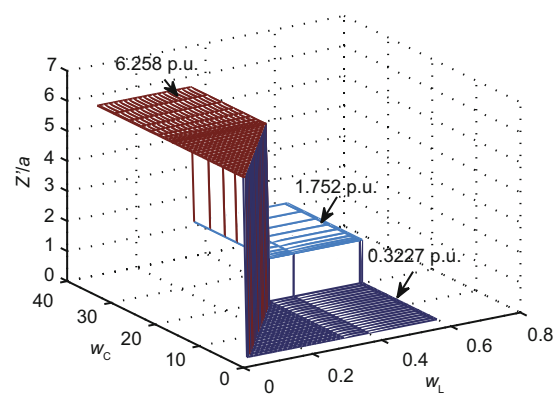


Fig. 13 Value of Z'/α for different ranges of w_L and w_C when $I_m=11$ kA

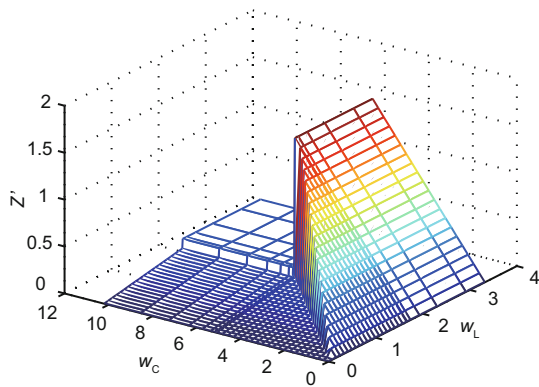


Fig. 14 Value of Z' for different ranges of w_L and w_C when $I_m=14$ kA

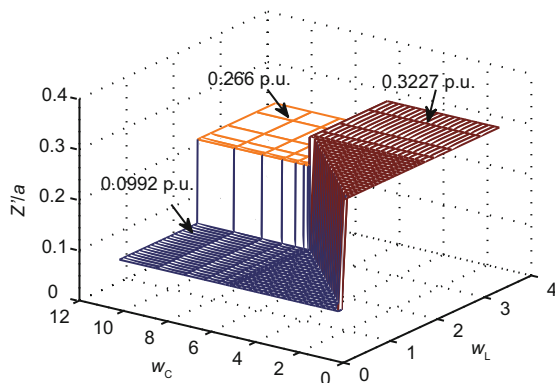


Fig. 15 Value of Z'/a for different ranges of w_L and w_C when $I_m=14$ kA

Table 4 The optimal value of FCL impedance and $|I_f^{3ph}|$ for $I_m=14$ p.u. according to different ranges of w_L and w_C

w_L	w_C	Z_{FCL} (p.u.)	$ I_f^{3ph} $ (p.u.)
>1.6604	>5.1012	0.266	13.16
<1.6604	$>3.0723w_L$	0.0992i	14
$>0.3255w_C$	<5.1012	$-0.3227i$	1.725

6 Conclusions

In this paper, the importance of FCL impedance optimization in a power network has been pointed out. The FCL impedance is a complex value and the FCL cost function is defined based on the costs of real and imaginary parts of FCL impedance. The fault current for each bus should be lower than I_m . The locus of FCL impedance is defined by the fault current being equal to or less than I_m .

By increasing the value of FCL impedance, the magnitude of the fault current is reduced and the costs

of FCL are increased. To determine the optimized value of FCL impedance, an objective function is defined to calculate the FCL impedance using the maximum reduction of fault current over a minimum cost of FCL. If the calculated FCL impedance cannot reduce the fault current to be equal to or less than I_m , according to the FCL impedance locus for I_m , FCL impedance is changed until the fault current reaches I_m .

The costs of FCL impedance include the costs of R_{FCL} , X_{FCL}^L , and X_{FCL}^C that can vary for different types of FCL. Thus, the FCL impedance optimization in the 14-bus IEEE system is conducted based on those cost variations.

The results show that the optimum FCL impedances for a different range of costs (including w_L and w_C) are different and that the FCL impedance can be any of pure R_{FCL} , pure X_{FCL}^L , or pure X_{FCL}^C depending on the range of costs. Note that in the test system, the combination of R_{FCL} , X_{FCL}^L , and X_{FCL}^C does not produce optimal results.

Because Z'/a is a fixed value for various costs of FCL, when θ is fixed, the changes in the costs can affect only the FCL impedance types and have no influence on the optimum value of FCL impedance. As a result, one can select the optimum FCL impedance value without considering the costs of FCL impedance.

References

- Abramovitz A, Smedley KM, 2012. Survey of solid-state fault current limiters. *IEEE Trans Power Electron*, 27(6): 2770-2782. <https://doi.org/10.1109/TPEL.2011.2174804>
- Alaraifi S, El Moursi MS, Zeineldin HH, 2013. Optimal allocation of HTS-FCL for power system security and stability enhancement. *IEEE Trans Power Syst*, 28(4): 4702-4711. <https://doi.org/10.1109/TPWRS.2013.2273539>
- Christie R, 2012. Power System Test Case Archive. https://www.ee.washington.edu/research/pstca/pf14/pg_tca14bus.htm
- Cvoric D, de Haan, SWH, Ferreira JA, et al., 2010. New three-phase inductive FCL with common core and trifilar windings. *IEEE Trans Power Del*, 25(4):2246-2254. <https://doi.org/10.1109/TPWRD.2010.2051688>
- Dam QB, Meliopoulos APS, 2006. Failure probability methodology for overdutied circuit breakers. 38th IEEE North American Power Symp, p.667-672. <https://doi.org/10.1109/NAPS.2006.359644>
- Dam QB, Meliopoulos APS, 2007. Reliability implications of increased fault currents and breaker failures. iREP Symp on Bulk Power System Dynamics and Control - VII.

- Revitalizing Operational Reliability, p.1-8.
<https://doi.org/10.1109/IREP.2007.4410540>
- Dam QB, Meliopoulos APS, Cokkinides GJ, 2013. A breaker-oriented fault analysis methodology. *Int Trans Electr Energy Syst*, 23(7):1071-1082.
<https://doi.org/10.1002/etep.1638>
- Didier G, Lévêque J, 2014. Influence of fault type on the optimal location of superconducting fault current limiter in electrical power grid. *Int J Electr Power Energy Syst*, 56:279-285. <https://doi.org/10.1016/j.ijepes.2013.11.018>
- Didier G, Bonnard CH, Lubin T, et al., 2015. Comparison between inductive and resistive sFCL in terms of current limitation and power system transient stability. *Electr Power Syst Res*, 125:150-158.
<https://doi.org/10.1016/j.epsr.2015.04.002>
- El Moursi MS, Hegazy R, 2013. Novel technique for reducing the high fault currents and enhancing the security of ADWEA power system. *IEEE Trans Power Syst*, 28(1): 140-148. <https://doi.org/10.1109/TPWRS.2012.2207746>
- Fotuhi-Firuzabad M, Aminifar F, Rahmati I, 2012. Reliability study of HV substations equipped with the fault current limiter. *IEEE Trans Power Del*, 27(2):610-617.
<https://doi.org/10.1109/TPWRD.2011.2179122>
- Guo Y, Yokomizu Y, Matsumura T, 2001. Design guidelines of a flux-lock superconducting fault current limiter with AC magnetic field coil for a 6.6-kV distribution system. *Electr Eng Jpn*, 135(4):17-25.
<https://doi.org/10.1002/ej.1038>
- Haghifam MR, Ghaderi A, Abapour M, 2009. Enhancement circuit breaker reliability by using fault current limiter. IEEE Power & Energy Society General Meeting, p.1-5.
<https://doi.org/10.1109/PES.2009.5275260>
- Hongesombut K, Mitani Y, Tsuji K, 2003. Optimal location assignment and design of superconducting fault current limiters applied to loop power systems. *IEEE Trans Appl Supercond*, 13(2):1828-1831.
<https://doi.org/10.1109/TASC.2003.812901>
- Hossen Heidary A, Radmanesh H, Fathi SH, et al., 2015. Series transformer based diode-bridge-type solid state fault current limiter. *Front Inform Technol Electron Eng*, 16(9):769-784. <https://doi.org/10.1631/FITEE.1400428>
- Javadi H, 2011. Fault current limiter using a series impedance combined with bus sectionalizing circuit breaker. *Int J Electr Power Energy Syst*, 33(3):731-736.
<https://doi.org/10.1016/j.ijepes.2010.11.023>
- Kim SY, Bae IS, Kim JO, 2010. An optimal location for superconducting fault current limiter considering distribution reliability. IEEE Power and Energy Society General Meeting, p.1-5.
<https://doi.org/10.1109/PES.2010.5588064>
- Kim SY, Kim WW, Kim JO, 2011. Evaluation of distribution reliability with superconducting fault current limiter. 10th IEEE Int Conf on Environment and Electrical Engineering, p.1-5.
<https://doi.org/10.1109/EEEIC.2011.5874570>
- Kim SY, Kim WW, Kim JO, 2012. Determining the location of superconducting fault current limiter considering distribution reliability. *IET Gener Transm Distr*, 6(3): 240-246. <https://doi.org/10.1049/iet-gtd.2011.0287>
- Kovalsky L, Yuan X, Tekletsadik K, et al., 2005. Applications of superconducting fault current limiters in electric power transmission systems. *IEEE Trans Appl Supercond*, 15(2): 2130-2133. <https://doi.org/10.1109/TASC.2005.849471>
- Matsumura T, Shimizu H, Yokomizu Y, 2001. Design guideline of flux-lock type HTS fault current limiter for power system application. *IEEE Trans Appl Supercond*, 11(1):1956-1959. <https://doi.org/10.1109/77.920235>
- Mukhopadhyay SC, Iwahara M, Yamada S, et al., 1998. Investigation of the performances of a permanent magnet biased fault current limiting reactor with a steel core. *IEEE Trans Magn*, 34(4):2150-2152.
<https://doi.org/10.1109/20.706833>
- Naderi SB, Jafari M, Tarafdar Hagh M, 2013. Parallel-resonance-type fault current limiter. *IEEE Trans Ind Electron*, 60(7):2538-2546.
<https://doi.org/10.1109/TIE.2012.2196899>
- Nagata M, Tanaka K, Taniguchi H, 2001. FCL location selection in large scale power system. *IEEE Trans Appl Supercond*, 11(1):2489-2494.
<https://doi.org/10.1109/77.920370>
- Saadat H, 1999. Power System Analysis. WCB/McGraw-Hill.
- Seo HC, Kim CH, Rhee SB, et al., 2010. Superconducting fault current limiter application for reduction of the transformer inrush current: a decision scheme of the optimal insertion resistance. *IEEE Trans Appl Supercond*, 20(4): 2255-2264. <https://doi.org/10.1109/TASC.2010.2048214>
- Shahriari SAA, Varjani AY, Haghifam MR, 2012. Cost reduction of distribution network protection in presence of distributed generation using optimized fault current limiter allocation. *Int J Electr Power Energy Syst*, 43(1): 1453-1459. <https://doi.org/10.1016/j.ijepes.2012.06.071>
- Stemmler M, Neumann C, Merschel F, et al., 2007. Analysis of unsymmetrical faults in high voltage power systems with superconducting fault current limiters. *IEEE Trans Appl Supercond*, 17(2):2347-2350.
<https://doi.org/10.1109/TASC.2007.899136>
- Teng JH, Lu CN, 2010. Optimum fault current limiter placement with search space reduction technique. *IET Gener Transm Distr*, 4(4):485-494.
<https://doi.org/10.1049/iet-gtd.2009.0340>
- Yamaguchi H, Kataoka T, 2007. Current limiting characteristics of transformer type superconducting fault current limiter with shunt impedance. *IEEE Trans Appl Supercond*, 17(2):1919-1922.
<https://doi.org/10.1109/TASC.2007.898494>
- Yousefi H, Aminifar F, Mirzaie M, 2016. Reliability assessment of HV substations equipped with fault current limiter considering changes of failure rate of components. *IET Gener Transm Distr*, 10(7):1504-1509.
<https://doi.org/10.1049/iet-gtd.2014.1250>